Towards a Virtual Functionally Graded Foam: Defining the rate independant constitutive response of a polymeric cellular solid as a function of density alone.

Stephen Kiernan[a], Michael D. Gilchrist[*,a],

[a]*School of Electrical, Electronic and Mechanical Engineering, University College Dublin, Ireland.*

Dedicated to Professor K. R. Rajagopal on the occasion of his 60th birthday.

Abstract

Functionally graded materials have been defined by Hirai [1] to be "a new generation of engineered materials wherein the microstructural details are spatially varied through a non-uniform distribution of the reinforcement phase(s)...". Extending this paradigm to the field of cellular solids, a functionally graded foam material (FGFM) may be thought of as a foam for which microstructural features such as cell size, and strut and wall (for closed cell foams) thickness vary in a continuous manner across the volume of the foam. These features may be varied globally by variation of the foam's density, ρ_{f}. Cui et al., [2] and Kiernan et al., [3] have shown some potential benefits of FGFMs under dynamic conditions using discretely layered Finite Element foam models. In their work the ABAQUS crushable foam model defines the constitutive response of each element layer of a regularly shaped specimen. The density, and corresponding Young's modulus, E^{f}, and hardening law of each layer is unique, thus defining a quasi-graded response. Motivated by their results, this paper attempts to describe the large strain compressive response of a generic foam, ultimately using ρ_{f} as the only independent input parameter. Experimental data is

[*]Corresponding author

Email addresses: stephen.kiernan@ucd.ie (Stephen Kiernan), michael.gilchrist@ucd.ie (Michael D. Gilchrist)

gathered from a number of expanded polystyrene foam specimens of different densities, and important foam characteristics are defined as functions of ρ_f. Results compare excellently to those of the ABAQUS foam model, and limitations of the modeling approach are discussed.
Key words: cellular, foam, constitutive, finite element, density, Abaqus

---

1. Introduction

Constitutive models or sets of equations that primarily relate the strain and stress tensor of a solid or fluid, exist for many types of materials of engineering or scientific importance, including metals, ceramics, soils, elastic, visco- and hyper-elastic solids (together with biological tissues) and, of course, cellular solids.

Once the initial investment of developing a new material model has been realised, there are many long term advantages to be gained from such robust and accurate equations instead of performing laboratory tests for which the experimental setup can be complicated, expensive and arduous. Parametric studies may be performed much more efficiently through simulation since there is no need to reset equipment and specimens between each test - batch programs may be defined simply to run automatically. Naturally, however, standard experimental testing of real world materials will always be required to provide data as input for all past and present material models.

Numerous constitutive relationships for cellular solids have been proposed and subsequently built upon since the middle of the last century. Early work by Rusch [4] expressed the relationship between the stress and strain of foam by the generalized equation:

$$\sigma = E^{\mathrm{f}} f(\varepsilon) \tag{1}$$

where $f(\varepsilon)$ is a generic non-linear function of strain. In Equation (1) the Young's modulus is assumed to be insensitive to the rate of strain. Building upon Equation (1), authors such as Meinecke and Schwaber [5], Nagy et al., [6], and Sherwood and Frost [7] have addressed the influence of strain rate, temperature and density on a foam's compressive response.

In what is now considered a classic work on the properties of cellular solids, Gibson and Ashby [8] present a comprehensive treatise on the subject of low density materials.

The general structure of cellular materials is described in detail, followed by some insights on the mechanics and properties of honeycombs, which can be viewed as two-dimensional foams. Three-dimensional foams are subsequently described, largely in terms of their mechanical, but to a lesser extent, thermal, electrical and acoustic properties also.

Due to their small volume fraction of solid material the deformation of cellular solids cannot be described by J2 plasticity theory; the volumetric component of deformation must be accounted for. Despande and Fleck [9] have developed two phenomenological isotropic models to account for this volumetric crushing. The first of these models assumes the yield surface to evolve in a geometrically self similar manner, i.e. the ratio of hydrostatic to deviatoric stress, σ_p / σ', remained constant, while the second allows for a change in shape of the yield surface due to differential hardening of σ_p and σ'. These models are widely cited; Despande and Fleck [10] have used the first to investigate the multi-axial yielding behaviour of ductile PVC foams, while Shahbeyk et al., [11] have also implemented this model in the form of a Vectorised User Material (`VUMAT`) subroutine in the ABAQUS/Explicit FE software while investigating the dynamic behaviour of metal foam filled square columns. An extension to Despande and Fleck's model was presented by Reyes et al., [12] while investigating the indentation and fracture behaviour of aluminium foam. They accounted for inhomogeneities through the foam in the model by including terms to describe statistical variations in the foam density. The five parameter model they use, following from the work of Hanssen et al., [13] is of the form:

$$\sigma = \sigma_{\text{yield}} + \beta\frac{\varepsilon}{\varepsilon_{\text{D}}} + \gamma\ln\left(\frac{1}{1-\left(\frac{\varepsilon}{\varepsilon_{\text{D}}}\right)^{\delta}}\right) \tag{2}$$

where $\varepsilon_D = 1 - \left(\frac{\rho^f}{\rho^s}\right)$, $\left(\frac{\varepsilon}{\varepsilon_D}\right)$ is a linear hardening term and $\gamma \ln\left(\frac{1}{1-\left(\frac{\varepsilon}{\varepsilon_D}\right)^{\delta}}\right)$ controls the non-linear strain hardening portion of the stress strain curve. The inclusion of ε_D in Equation (2) ensures that there is a strong coupling between the evolution of the strain hardening with the actual change in foam density during foam compaction. To account for the statistical variation in density a mean value and standard deviation of ρ^f, taken from the data base of Hanssen et al., [13] was also given as input parameters. It was found, however, that the inclusion of this variation had little impact on the results of the study.

More recently Bouix et al., [14] have also noted the importance of foam density on dynamic deformations. Quasi-static (0.01 s^{-1}) and dynamic ($\approx$ 200 s^{-1}) compression tests using electromechanical and modified flywheel devices respectively, were performed on EPP specimens and showed ρ^f to be a significant factor in influencing the $\sigma_{engineering} - \varepsilon_{true}$ curves obtained by the authors. Indeed an increase in ρ^f from 35 kg/m^3 to 150 kg/m^3 showed more than an eight fold increase in yield stress. Similar results were also seen at strain rates of 1500 s^{-1} using a Split Hopkinson Pressure Bar apparatus. At quasi-static strain rates results compared well with Equation (3) by Gibson and Ashby [8], which relates the Young's modulus of a part open / part closed cell foam to its density by:

$$\frac{E^f}{E^s} \approx C_1 \left(\phi \frac{\rho^f}{\rho^s}\right)^2 + C_2(1-\phi)\left(\frac{\rho^f}{\rho^s}\right) \tag{3}$$

where ϕ is the fraction of material contained in the cell struts and C_1 and C_2 are constants of proportionality. It is important to note however that for the same bulk density, the foam microstructure on a cellular scale will play an important role in determining salient properties.

Liu and Subhash [15] have proposed a simple phenomenological constitutive model that is capable of capturing the tensile and compressive response of low density foams.

This six parameter model takes the form:

$$\sigma = A\frac{e^{\alpha\varepsilon}+1}{B+e^{\beta\varepsilon}} + e^{C}(e^{\gamma\varepsilon}-1) \tag{4}$$

The parameter A is a scaling factor which controls the overall magnitude of the curve on the stress axis (for example, with increasing initial foam density), while α and β control the hardening / softening behaviour of the stress-strain curve. B controls the onset of plasticity under compression and the expression $e^{C}(e^{\gamma\varepsilon}-1)$ defines the rapid increase in stress during the densification stages of compressive deformation. Although this model is quite simple, the authors do concede that determining the necessary parameters is not a simple task. In spite of the fact that this model is quite versatile in accurately describing the full uniaxial deformation curve of a multitude of foams for arbitrary initial densities, it should be noted that this model is essentially a multi-variable function which is *a posteriori* fitted to experimental data to describe the stress-strain behaviour of a cellular solid of a given initial density. In this way the model of Equation (4) has no physical connection to the underlying mechanisms involved in foam deformation.

While the models discussed above are each successful for their intended applications they are unsuitable to be placed within the framework of a graded element formulation; some have an excessive number of input variables, while others are only one - dimensional. It is a necessity that a proposed model ultimately be reliant on a single input parameter; authors such as Santare and Lambros [16], Kim and Paulino [17], and Zhang and Paulino [18] have developed two - dimensional elastically graded elements in which there are only one or two grading parameters such as E, υ^{el} or ρ. This paper attempts to develop a three - dimensional cellular constitutive model for which the only independent variable is the density; all other influencing variables will be defined as functions of ρ_{f}. As part of future work this model will then be integrated into a three - dimensional graded finite element formulation in which density is the grading parameter. In this way a continuously graded

F.E. cellular response may be described. The presented model is based on a selection of isotropic closed cell expanded polystyrene (EPS) specimens under monotonic compressive loading, and as such in its current form is not applicable to honeycomb structures or ceramic / metallic foams where brittle fracture may occur.

Section 2 of this paper first describes the experimental data obtained, followed by the constitutive equations and geometries describing the newly proposed model in Sections 3 and 4. Results under static and dynamic loading conditions followed by their discussion are presented in Section 6, followed finally by concluding remarks in Section 7.

2. Experimental Testing

In order to obtain the necessary data for the proposed constitutive model, a series of quasi-static compression tests at a strain rate of 0.001/s were performed on EPS foam specimens of densities 15, 20, 25, 50 and 64 kg/m^3. The assumption of a vanishing Poisson's ratio for low density EPS foam was validated in tests up to 95% compressive strain, which showed lateral strains to be less than 2%. A model by Schraad and Harlow [19], in which the finite compressive stress strain response of low density foam is described by stochastic material representations, is used to curve fit the experimental data as shown in Figure 1. In their model the finite compressive strain is related to stress by a finite strain Young's modulus, $E^{\mathrm{f}}(\varepsilon)$. $E^{\mathrm{f}}(\varepsilon)$ is itself dependent on the stiffness (E^{s} =3.3 GPa) and density (ρ^{s} =1050 kg/m^3) of the solid EPS, $\rho^{\mathrm{f}}(\varepsilon)$, and a shape factor $A(\varepsilon)$, and is given by:

$$E^{\mathrm{f}}(\varepsilon) = A(\varepsilon)E^{\mathrm{s}}\left(\frac{\rho^{\mathrm{f}}}{\rho^{\mathrm{s}}}\right)^2 \tag{5}$$

where $A(\varepsilon)$ is given by:

$$
\begin{aligned}
A(\varepsilon) \;=\; & \frac{A_0}{2}\left\{1-\mathrm{erf}\left(\frac{\varepsilon_{\mathrm{y}}-\varepsilon}{\sqrt{2}\sigma_{\varepsilon_{\mathrm{y}}}}\right)\right\} \\
+\; & \frac{A_1}{2}\left\{1-\mathrm{erf}\left(\frac{\varepsilon-\varepsilon_{\mathrm{y}}}{\sqrt{2}\sigma_{\varepsilon_{\mathrm{y}}}}\right)\right\} \\
+\; & \frac{A_2-A_1}{2}\left\{1-\mathrm{erf}\left(\frac{\varepsilon-\varepsilon_{\mathrm{D}}}{\sqrt{2}\sigma_{\varepsilon_{\mathrm{D}}}}\right)\right\}
\end{aligned} \tag{6}
$$

and erf(x) is the error function defined by:

$$
\mathrm{erf}(x) \;=\; \frac{2}{\sqrt{\pi}}\int_0^x \mathbf{e}^{-t^2}dt \tag{7}
$$

$$
\;=\; \frac{2}{\sqrt{\pi}}\sum_{n=0}^{\infty}\frac{(-1)^n x^{2n+1}}{(2n+1)n!} \tag{8}
$$

ε_y and ε_D are the values of the yield and densification strain respectively. $\sigma_{\varepsilon_{\mathrm{y}}}$ and $\sigma_{\varepsilon_{\mathrm{D}}}$ are the standard deviations of ε_y and ε_D and provide a measure for the spread of ε across ε_y and ε_D. A_0, A_1 and A_2 are constants of proportionality which are fitted to the experimental stress - strain response of the 64kg/m^3 $EPS, and influence the slope of the linear elastic, plateau stress, and dens$ $E^{\mathrm{f}}(\varepsilon)\varepsilon$. For EPS with ρ_{f} = 64kg/m^3 Table 1 shows the parameters used to calibrate Schraad and Harlow's model. Figure 1 compares the predictions of this model to that of the experimental results. For densities other than 64kg/m^3 the scaling parameter ($64/\rho_{\mathrm{f}}$) was found to give a good fit up to true strains of -1.5 for the set of experiments carried out. Although closed cell isotropic EPS foams were used to calibrate this model, due to the calibration method other types of foams would equally be suitable, since the model is intended to represent the global response of a generic foam. For example, were open cell expanded polyurethane (EPU) foams used instead of closed cell EPS, the curve fitting phase of calibration would simply account for the finite strain response of the EPU by adjusting the equation of Figure 1 and values of Table 1. In this way, although there are qualitative differences between open and closed cell foams, due to unique geometric features on a cell by

cell level, on a global scale $\partial\sigma/\partial\varepsilon$ will be captured by the curve fit through recalibration regardless of whether an open or closed cell foam is used.

The relationship between the Young's modulus and density for EPS, shown in Figure 2, is well described by Equation (3), for which $C_1 = 385.58$, $C_2 = 556.87$, and $\phi = 0.68$. This relationship is also well described by a linear fit of $E^f = 0.1943\rho_f$ - 0.1983. It is important to note that following initial calibration of $E^f(\rho_f)$ and the values of Table 1, the numerical curves of Figure 1 were generated simply by varying ρ_f. Following from Cui et al., [2] and Kiernan et al., [21], curves of higher density foams may subsequently be extrapolated using this method.

3. Constitutive Response

The proposed constitutive model is based loosely on the model of Despande and Fleck [9], which is implemented as the crushable foam model for both open and closed cell foams available in the ABAQUS [20] material library. However, it differs largely in the manner in which the plastic hardening behaviour is defined, and will use the methodology behind the numerical results of Section 2. The Lamé constants of the elastic stiffness matrix for a cellular solid can be expressed as:

$$\lambda_1 = \frac{E^f(1-\upsilon^{el})}{(1-2\upsilon^{el})(1+\upsilon^{el})} \tag{9}$$

$$\lambda_2 = \frac{E^f}{2(1+\upsilon^{el})} \tag{10}$$

$$\sigma_{ij}^{el} = C_{ijkl}^{el}(\varepsilon_{kl} - \varepsilon_{kl}^{pl}) \tag{11}$$

where $C_{ijkl}^{el} = \left(\frac{3\lambda_1+2\lambda_2}{3}\right)\delta_{ij}\delta_{kl} + \lambda_2(\delta_{ik}\delta_{jl} + \delta_{il}\delta_{jk} - \frac{2}{3}\delta_{ij}\delta_{kl})$ is the material stiffness tensor possessing both minor and major symmetries ($C_{ijkl}^{el} = C_{ijlk}^{el} = C_{jikl}^{el} = C_{klij}^{el}$). δ_{ij} is the Kronecker delta and υ^{el} is the the elastic Poisson's ratio. At small strains Equations (9), (10) and (11)

are adequate at capturing the linear elastic behaviour of foams, and so the influence of cellular voids may be neglected. However at large strains these voids become integral to understanding a foam's deformation response. They possess a dependency on hydrostatic stress and so a multi-axial equivalent stress that considers both shear and normal components of stress should be used. The ABAQUS crushable foam model defines for a foam under multiaxial loading, the equivalent stress σ_{equiv} as:

$$\sigma_{\text{equiv}} = \sqrt{\sigma_e^2 + \alpha^2(\sigma_{\text{p}} - \sigma_{\text{p}}^0)^2} \tag{12}$$

where σ_e is the J2 von Mises stress given by:

$$\sigma_e = \sqrt{\frac{3}{2}\sigma'_{ij}\sigma'_{ij}} \tag{13}$$

σ_{p} is the hydrostatic pressure term:

$$\sigma_{\text{p}} = -\frac{1}{3}\sigma : \mathbf{I} \tag{14}$$

and the deviatoric stress σ' is given by:

$$\sigma' = \sigma + \sigma_{\text{p}} \tag{15}$$

$\sigma_{\text{p}}^0 = \frac{p_c^0 - p_t}{2}$ defines the centre of the yield ellipse along the pressure-axis of the foam's yield surface and the superscript 0 denotes initial conditions. p_c and p_t are the hydrostatic yield stress in compression and tension respectively.

3.1. Yielding

Deformation will continue elastically until σ_{equiv} reaches some value $\sigma_{\text{yield}} \in \partial\mathbb{E}_\sigma$, where $\partial\mathbb{E}_\sigma$ denotes the yield surface of the elastic domain. The elastic domain, $\mathbb{E}_\sigma \subset \mathbb{R}^3$, is composed of $\partial\mathbb{E}_\sigma \cup \text{int}(\mathbb{E}_\sigma)$ and can be expressed as:

$$\mathbb{E}_\sigma = \{x := (\sigma_{\text{ij}}, p_c) \in \mathbb{R} \times \mathbb{R} \mid f(x) \leq 0\} \tag{16}$$

Various yield criteria exist for porous materials (see Schreyer et al., [22] and Despande and Fleck [10]). In this model, similarly to the ABAQUS foam model of Figure 3, plastic yielding begins when σ_{equiv} reaches σ_{yield}:

$$\begin{aligned} f(\sigma_{\text{ij}}, p_c) &= \sigma_{\text{equiv}} \\ &\quad - \sigma_{\text{yield}} \\ &= \sqrt{\sigma_e^2 + \alpha^2(\sigma_{\text{p}} - \sigma_{\text{p}}^0)^2} \\ &\quad - \alpha\tfrac{p_c + p_t}{2} \end{aligned} \tag{17}$$

α defines the aspect ratio of the yield surface, which has an elliptical dependence on the deviatoric stress, σ', and on the pressure stress, σ_{p}. Despande and Fleck [9] show that α may be calculated from knowledge of the plastic Poisson ratio υ^{pl} by:

$$\upsilon^{\text{pl}} = -\frac{\dot{\varepsilon}_{11}^{\text{pl}}}{\dot{\varepsilon}_{33}^{\text{pl}}} = \frac{\frac{1}{2} - \left(\frac{\alpha}{3}\right)^2}{1 + \left(\frac{\alpha}{3}\right)^2} \tag{18}$$

Solving for α in terms of υ^{pl} gives

$$\alpha = \pm\frac{3\sqrt{-(2\upsilon^{\text{pl}} + 2)(2\upsilon^{\text{pl}} - 1)}}{2(\upsilon^{\text{pl}} + 1)} \tag{19}$$

For low density foams, if υ^{pl} is assumed to be zero then α reduces to $\frac{3\sqrt{2}}{2}$. α may also be calculated from knowledge of the ratios of yield in uniaxial and hydrostatic compression, and hydrostatic tension and compression:

$$\alpha = \frac{3k}{\sqrt{(3k_t + k)(3 - k)}} \tag{20}$$

for which:

$$k = \frac{\sigma_{\text{yield}}}{p_c^0} \quad \text{and} \quad k_t = \frac{p_t}{p_c^0} \tag{21}$$

Following the ABAQUS documentation, for low density foams k and k_t are chosen to be 1.1 and 0.1 respectively.

3.2. The Plastic Flow Potential

Following yield, further deformation occurs in a plastic / non-recoverable manner. The normality hypothesis of plasticity allows for the determination of what direction this flow takes place in, i.e. the values of the plastic strain tensor components. For low density solids flow is typically non-associative - the direction of plastic flow (increment in the plastic strain tensor) is not the same as the normal to the tangent of the yield surface at the point of loading and so the non-associative flow potential, G, is given by:

$$\begin{aligned} G(\sigma_{\text{ij}}) &= \sqrt{\sigma_e^2 + \alpha^2 \sigma_p^2} \\ &= \sqrt{\sigma_e^2 + \frac{9}{2}\sigma_p^2} \end{aligned} \tag{22}$$

The shape of $G(\sigma_{\text{ij}})$ is shown in Figure 4. The plastic strain increment, $d\varepsilon^{\text{pl}}$, for volumetric hardening may then be calculated from the plastic flow rule:

$$d\varepsilon_{\text{ij}}^{\text{pl}} = d\lambda \left(\frac{\partial G}{\partial \sigma_{\text{ij}}} \right) \tag{23}$$

The derivatives, $\dfrac{\partial G}{\partial \sigma_{ij}}$, are explicitly given as:

$$\frac{\partial G}{\partial \sigma_{ij}} = \frac{3\sigma_{ij}}{\sqrt{6(\sigma_{\text{ij}} : \sigma_{\text{ij}})}} \tag{24}$$

3.3. The Plastic Multiplier

If the flow potential is viewed as containing the directions of the plastic strain tensor then the plastic flow multiplier, $d\lambda$ is a scalar value which defines the magnitude of this direction. The ABAQUS crushable foam model defines $d\lambda$ equal to $\frac{\sigma : \mathrm{d}\varepsilon^{\mathrm{pl}}}{G}$, where $\mathrm{d}\varepsilon^{\mathrm{pl}} = \mathrm{d}\lambda\frac{d\sigma}{dG}$. These equations appear dependent on one another, i.e. prior knowledge of either $\mathrm{d}\lambda$ or $\mathrm{d}\varepsilon^{\mathrm{pl}}$ seems to be required and so instead the plastic multiplier is defined as follows. $d\lambda$ can be found from the consistency condition, i.e. the requirement that, for rate independent plasticity at least, during plastic deformation the current stress remains on the yield surface. From Equation (17) then, for an increment in plastic strain $d\varepsilon^{\mathrm{pl}}_{\mathrm{ij}}$, the subsequent yield surface $f(\sigma_{\mathrm{ij}} + d\sigma_{\mathrm{ij}}, p_c + dp_c)$ equals $f(\sigma_{\mathrm{ij}}, p_c) + df = 0$. df can be written as:

$$df = \frac{\partial f}{\partial \sigma} : d\sigma + \frac{\partial f}{\partial p_c} : dp_c = 0 \tag{25}$$

Substituting Equation (11) into Equation (25) and noting that $d\varepsilon^{\mathrm{pl}} = d\lambda\frac{\partial G}{\partial \sigma}$ gives:

$$\frac{\partial f}{\partial \sigma} : C : d\varepsilon - \frac{\partial f}{\partial \sigma} : C : d\lambda\frac{\partial G}{\partial \sigma} + \frac{\partial f}{\partial p_c}dp_c = 0 \tag{26}$$

Rearranging for $d\lambda$ then gives an explicit expression for the flow multiplier increment:

$$d\lambda = \frac{\dfrac{\partial f}{\partial \sigma_{\mathrm{ij}}} : C_{\mathrm{ijkl}} : d\varepsilon_{\mathrm{kl}} + \dfrac{\partial f}{\partial p_c}dp_c}{\dfrac{\partial G}{\partial \sigma_{\mathrm{ij}}} : C_{\mathrm{ijkl}} : \dfrac{\partial f}{\partial \sigma_{\mathrm{kl}}}} \tag{27}$$

Substituting Equation (27), and $\frac{\partial G}{\partial \sigma}$, into (11) gives the final expression for the stress tensor as:

$$\sigma^{\mathrm{el}}_{\mathrm{ij}} = C^{\mathrm{el}}_{\mathrm{ijkl}}\left(\varepsilon_{\mathrm{kl}} - \left(\frac{\dfrac{\partial f}{\partial \sigma_{\mathrm{ij}}} : C^{\mathrm{el}}_{\mathrm{ijkl}} : d\varepsilon_{\mathrm{kl}} + \dfrac{\partial f}{\partial p_c}dp_c}{\dfrac{\partial G}{\partial \sigma_{\mathrm{ij}}} : C^{\mathrm{el}}_{\mathrm{ijkl}} : \dfrac{\partial f}{\partial \sigma_{\mathrm{kl}}}}\right)\frac{\partial G}{\partial \sigma_{\mathrm{ij}}}\right) \tag{28}$$

The stress derivatives of the yield function, $\frac{\partial f}{\partial \sigma_{ij}}$ are explicitly given as:

$$\frac{\partial f}{\partial \sigma_{ij}} = \begin{cases} \dfrac{12(\sigma_{ij} + \sigma_p^0)}{4\sqrt{6(\sigma_{ij} : \sigma_{ij}) + 12\sigma_p^0(\sigma_{ij} : \mathbf{I}) + \left(2\alpha\sigma_p^0\right)^2}} \\ \text{...if i = j} \\ \dfrac{3\sigma_{ij}}{\sqrt{6(\sigma_{ij} : \sigma_{ij}) + 12\sigma_p^0(\sigma_{ij} : \mathbf{I}) + \left(2\alpha\sigma_p^0\right)^2}} \\ \text{...if i} \neq \text{j} \end{cases} \tag{29}$$

and $\frac{\partial f}{\partial p_c}$ is a scalar value given by:

$$\frac{\partial f}{\partial p_c} = \frac{3(\sigma_{ij} : \mathbf{I}) + 9\sigma_p^0}{\sqrt{24(\sigma_{ij} : \sigma_{ij}) + 48\sigma_p^0(\sigma_{ij} : \mathbf{I}) + \left(2\alpha\sigma_p^0\right)^2}} - \frac{3\sqrt{2}}{4} \tag{30}$$

3.4. Strain Hardening / Cell Densification

At strains exceeding ε_{yield} volumetric compaction of the foam occurs and p_c expands, while p_t remains constant. This is shown in Figure 4 and described by Equation (31) as [20]:

$$p_c\left(\varepsilon_{vol}^{pl}\right) = \sigma_c\left(\varepsilon_{axial}^{pl}\right)\left(\frac{\sigma_c\left(\varepsilon_{axial}^{pl}\right)\left(\frac{1}{\alpha^2} + \frac{1}{9}\right) + \frac{p_t}{3}}{p_t + \frac{\sigma_c\left(\varepsilon_{axial}^{pl}\right)}{3}}\right) \tag{31}$$

Typically the expression $\sigma_c\left(\varepsilon_{axial}^{pl}\right)$ is provided in tabular form to the ABAQUS crushable foam model and is obtained from a uni-axial quasi static compression test. However, it has already been shown in Section 2 that through the use of the model by Schraad and Harlow [19] it is possible to specify an approximate $\sigma_c\left(\varepsilon_{axial}^{pl}\right)$ curve from knowledge of ρ_f.

3.5. Other Parameters

Once the finite stress - strain behaviour has been fully defined, other important parameters can be determined. For example it is often of interest to know the absorbed energy (ψ), foam efficiency (φ), and foam ideality (ι), which can be important parameters in describing the energy absorbing effectiveness of foam structures. These are defined, respectively as:

$$\psi = \int_0^{\varepsilon} \sigma : \varepsilon \, \mathrm{d}\varepsilon \tag{32}$$

$$\varphi = \frac{\int_0^{\varepsilon} \sigma : \varepsilon \, \mathrm{d}\varepsilon}{\sigma} \tag{33}$$

$$\iota = \frac{\int_0^{\varepsilon} \sigma : \varepsilon \, \mathrm{d}\varepsilon}{\sigma : \varepsilon} \tag{34}$$

4. Finite Element Geometry

A single 8-node linear hexahedral, reduced integration element (C3D8R) with hourglass control and prescribed displacement boundary conditions is used to validate the model under static compression conditions. Figure 5 shows the element assembly used to validate the model under dynamic conditions. A total of 1125 C3D8R elements are used to define the specimen geometry and C3D8R elements define the striker platen. The platen is constitutively defined with a linear elastic steel definition (E = 210GPa, ρ = 7900kg/m^3), although these properties are superseeded by a rigid body tie constraint, which is applied to the elements of the platen to eliminate any deformation that may otherwise occur, and reduce the computational time.

The specimen is impacted by the striker at two speeds of 5.4 and 7.7m/s in the negative z-direction. These speeds are taken from the equestrian certification test standards

EN1384:1996 [23] and EN14572:2005 [24] respectively, and have previously been chosen by Forero Rueda et al., [25] and Cui et al., [26] while investigating the energy absorbing performance of virtually graded equestrian helmet liners. Arbitrarily chosen densities of 40, 50, 64, 84, and 104kg/m^3 are assigned to the virtual foam in order to test the proposed model. The corresponding initial foam moduli were computed within the `VUMAT` from Equation (3). The bottom of the specimen is contrained from moving in the z-direction and the striker is constrained to move only in the z-direction. Contact is defined using a kinematic contact formulation, with a tangential coefficient of friction of zero. The ABAQUS/Explicit solver is used in all simulations.

5. Model Validation

The equations of Section 2 and 3 are now coded and numerically integrated in the ABAQUS subroutine `VUMAT` and validated under simulated static and dynamic compression loadings against identical simulations using the ABAQUS crushable foam model. All simulations using the crushable foam model will be henceforth know as '`HEX`', while simulations using the newly proposed model will be referred to as '`VUMAT`'.

5.1. Displacement controlled compression

A single C3D8R element is used to validate the proposed model under prescribed displacement boundary conditions. Its dimensions are 0.5m^3. The four nodes of the bottom face are constrained in the vertical direction while a velocity boundary condition of -0.425 m·s^{-1} is applied to nodes of the top face, giving a simulation time of 1 second. Although this is intended to simulate a static compression test the simulations were carried out using the ABAQUS/Explicit solver, which is typically used for time scales on the order of 10^{-6} - 10^{-2} seconds. As strain rate effects were not considered, the displacement controlled velocity of the striker will not influence the response of either model.

5.2. Acceleration Management

The geometry assembly as shown in Figure 5 is used to model a simple cushioning structure. `HEX` and `VUMAT` models are both used as the material definition - this is to determine whether the `VUMAT` is capable of capturing a dynamic response and also its stability under general contact problems. Two striker velocities of 5.4 and 7.7m/s were simulated.

6. Results and Discussion

Figures 6(a) - 6(d) show the static compressive response of the `HEX` model compared to that of the `VUMAT` user model. A number of important foam response characteristics are computed, including absorbed energy, foam efficiency, and foam ideality (Equations (32) - (34)). Figure 6(a) shows the Gauss point stresses are well captured up to a finite true strain of -1.897 ($\varepsilon_{\text{engineering}} = 0.85$) for virtual foams of densities ranging from 40 kg/m^3 - 104 kg/m^3, and unloading is assumed to be linear with the same slope as the initial Young's modulus, i.e. viscoelastic effects are not considered in either model. This is a reasonable limiting assumption under dynamic conditions since viscoelastic effects typically occur over a time scale far greater than that of a cushioning impact. Figures 6(b) - 6(d) show the absorbed energy, efficiency and ideality response of these virtual foams. Since these important cushioning characteristics are all derived directly from the constitutive response (Equations (32) - (34)), it is not surprising that the `VUMAT` is quite capable of accurately capturing their response curves also.

Figures 7(a) - 7(e) compare the `VUMAT`'s ability to model the acceleration - time response of a standard dynamic impact simulation against that of the `HEX` model. Five foam densities for $\upsilon^{\text{el}} = 0.0$, simulated under two impact velocities are presented. Globally both models respond almost identically; in each Figure both the period of each impact and the

time of peak acceleration are very closely matched. However, the VUMAT does exhibit a small amount of noise near the beginning of the plateau region of acceleration. A possible reason for this is the fact that a small amount of Rayleigh damping is defined within the HEX model, while no damping of any kind is present in the VUMAT. Since force is directly proportional to acceleration and the total impact time of the VUMAT (time between which acceleration is greater than 0 m/s^2) is almost identical to that of the HEX, it is a good indicating that globally at least, nodal forces are being calculated and transmitted through the assembly in a consistent manner.

Despite the accuracy of this VUMAT when compared to results of the HEX, two limitation can be identified. Firstly, the computational time required to run each simulation is quite large. Table 2 shows the CPU solving time, stable time increment and number of increments required. While the ABAQUS foam model is computationally efficient, requiring a CPU time of 6 seconds to simulate an impact with a 104kg/m^3 foam, this number rising to 7 seconds for a 40kg/m^3 foam, a CPU time of about 40 minutes for a 40kg/m^3 foam is needed for the VUMAT to perform the same simulation. In addition to the fact that the ABAQUS foam model is a commercial quality code and so should be expected to be quite efficient, it is supposed that the reason for the VUMAT's relative sluggishness lies in the computation of the hardening response of the foam. During each call to the VUMAT by ABAQUS 1005 real values are calculated for the components of the array containing the $\sigma - \varepsilon$ curve that is generated by ρ_f. ABAQUS may call the VUMAT for up to 136 elements and thus for a single time increment, roughly 8300 calculations are performed ((1125*1005) / 136) in defining the hardening curve for the entire specimen assembly alone.

Secondly, the curve fitting methodology outlined in Section 2 may be interpreted as a more qualitative representation of a closed cell EPS foam's hardening response as ρ_f is removed more from the calibration value of 64kg/m^3. However, the primary purpose of

this model is to be integrated as the constitutive response of a finite element in which ρ^f is varied spatially, thus defining an FGFM. Is is for this reason that the constitutive response by ultimately dependent on ρ_{f} alone; this methodology provides a realistic trend of the global response of a foam's compressive behaviour over a finite range of densities as seen from Figure 1.

6.1. Model Robustness

Although results presented here are based on a selection of EPS specimens with $\upsilon^{\mathrm{el}} = 0.0$, values of 0.1 and 0.2 with $\rho_{\mathrm{f}} = 50\mathrm{kg/m}^3$ were also simulated purely to test the robustness of the model. This is because some variables of Equation (27) equate to zero for $\upsilon^{\mathrm{el}} = 0$. However, it is not physically consistent to simply change υ^{el}; the Poisson's ratio is a structural parameter and any change in its value in reality would be the result of a change in the foam's microstructure. Indeed, the definition of the yield surface and hardening response is based on the assumption that $\upsilon^{\mathrm{el}} = 0$. Therefore, unlike results for which $\upsilon^{el} = 0$, for $\upsilon^{el} > 0$ results should not be considered a realistic representation of the EPS response.

It was found that under both static and dynamic loading increasing υ^{el} had no significant influence on either model; comparing Figure 8 to Figure 7(b) shows the period and peak values to be quite similar. However, increased fluctuations in acceleration can be seen in the `HEX` for $v = 5.4$, indicating that υ^{el} may have a more physical meaning within the `HEX` than the `VUMAT`. The CPU solver time in all simulations was seen to increase with increasing Poisson's ratio also.

By generating a $\sigma - \varepsilon$ curve within the source code, along with a number of other necessary parameters, the proposed `VUMAT` requires the user to only specify an initial foam density for complete calibration of the model. Table 3 highlights explicitly the input parameters required for each model.

7. Conclusions

- A new constitutive model for a uniform isotropic cellular solid has been developed and coded as a `VUMAT` by integrating the model proposed by Schraad and Harlow [19] with that of Despande and Fleck [9], the latter of which is implemented in the ABAQUS F.E. software and widely known as the ABAQUS crushable foam model.

- The advantage of this `VUMAT` lies in the fact that only a single parameter, the initial foam density ρ^{f} is required as an input. All other parameters are calculated within the `VUMAT` source code as functions of ρ^{f} and require no input from the user. Such functions are derived from experimental testing on closed cell EPS specimens. This is in contrast to a tabulated full true stress - true plastic strain curve, which is typically required as input to the `HEX` model, in addition to other parameters such as $E^{\mathrm{f}}, \rho^{\mathrm{f}}, p_c$, and p_t. Using the model of Schraad and Harlow [19] it possible to generate these parameters, and a full, experimentally validated, $\sigma_{\mathrm{true}} - \varepsilon^{\mathrm{pl}}_{\mathrm{true}}$ curve from ρ^{f} alone. Similarly to the crushable foam model, the proposed model also uses this $\sigma_{\mathrm{true}} - \varepsilon^{\mathrm{pl}}_{\mathrm{true}}$ data to define the hardening law and evolution of the yield surface $\partial\mathbb{E}_{\sigma}$.

- The `VUMAT` however is computationally inefficient (see Table 2). It is speculated that this is due to the large number of floating point computations required to calculate the hardening $\sigma - \varepsilon$ curve for each integration point at every time increment. Also it is unknown how the ABAQUS foam model uses the tabular $\sigma - \varepsilon$ data it requires as input, however as it is a code of commercial quality it is assumed to be highly optimised.

- Although predicting a foam's constitutive response by explicitly availing of other variables would increase the model's accuracy if a particular density were being investigated, the model is required to provide good prediction of the foam's response

over a range of densities. The prediction need not be exact at every density, but it should be qualitatively realistic. Results from Section 2 show that the model does achieve this over the finite range of densities investigated.

- This model is intended as a first step towards developing a three - dimensional functionally graded cellular constitutive law that may predict the hypothesised global dynamic response of an FGFM. This would build upon the work already carried out by Cui et al., [2] and Kiernan et al., [3]. While the methodology outlined in this paper appears to achieve global results quite similar to those of the `HEX` model while using only one independent input parameter, it is unlikely to be a successful method when studying the local deformation of a foam on a cellular scale. ρ_{f} is only a good indicator of response on a global scale when the contribution of many cells can be statically viewed as homogeneous; on a microstructural scale geometric characteristics such as non-uniform ligament cross sectional area, material concentration at vertices and local anisotropy should be accounted for explicitly. Jang et al., [27] investigate such influences in detail.

References

[1] T. Hirai, Functionally Gradient Materials. VCH Verlagsgesellschaft mbH Publishers (1996).

[2] L. Cui, S. Kiernan, M.D. Gilchrist, Designing the energy absorbing capacity of functionally graded foam materials. Materials Science and Engineering A 507 (2009) 215 - 225.

[3] S. Kiernan, L. Cui, M.D. Gilchrist, Propagation of a stress wave through a function-

ally graded foam. International Journal of Non-Linear Mechanics 44 (2009) 456 - 468.

[4] K.C. Rusch, Load-compression behaviour of flexible foams. Journal of Polymer Science 13 (1969) 2297 - 2311.

[5] E.A. Meinecke, D.M. Schwaber, Energy absorption in polymeric foams. I. Prediction of impact behavior from Instron data for foams with rate-independent modulus. Journal of Applied Polymer Science 14 (1970) 2239 - 2248.

[6] A. Nagy, W.L. Ko, U.S. Lindholm, Mechanical behavior of foamed materials under dynamic compression. Journal of Cellular Plastics 10 (1974) 127 - 134.

[7] J.A. Sherwood, C.C. Frost, Constitutive modeling and simulation of energy absorbing polyurethane foam under impact loading. Polymer Engineering Science 32 (1992) 1138 - 1146.

[8] L.J. Gibson, M.F. Ashby, Cellular Solids: Structures and Properties - 2nd edition. Cambridge University Press (1997).

[9] V.S. Despande, N.A. Fleck, Isotropic constitutive models for metallic foams. Journal of the Mechanics and Physics of Solids 48 (2000) 1253 - 1283.

[10] V.S. Despande, N.A. Fleck, Multi-axial yield behavior of polymer foams. Acta Materialia 49 (2001) 1859 - 1866.

[11] S. Shahbeyk, N. Petrinic, A. Vafai, Numerical modelling of dynamically loaded metal foam-filled square columns. International Journal of Impact Engineering 34 (2007) 573 - 586.

[12] A. Reyes, O.S. Hopperstad, T. Berstad, A.G. Hanssen, M. Langseth, Constitutive modeling of aluminum foam including fracture and statistical variation of density. European Journal of Mechanics - A/Solids 22 (2003) 815 - 835.

[13] A.G. Hanssen, O.S. Hopperstad, M. Langseth, H. Ilstad, Validation of constitutive models applicable to aluminium foams. International Journal of Mechanical Sciences 44 (2002) 359 - 406.

[14] R. Bouix, P. Viot, J.L. Lataillade, Polypropylene foam behaviour under dynamic loadings: Strain rate, density and microstructure effects. International Journal of Impact Engineering 36 (2009) 329 - 342.

[15] Q. Liu, G. Subhash, A phenomenological constitutive model for foams under large deformations. Polymer Engineering Science 44 (2004) 463 - 473.

[16] M.H. Santare, J. Lambros, Use of graded finite elements to model the behavior of nonhomogeneous materials. Journal of Applied Mechanics 67 (2000) 819 - 822.

[17] J.H. Kim, G.H. Paulino, Isoparametric graded finite elements for nonhomogeneous isotropic and orthotropic materials. Journal of Applied Mechanics 69 (2002) 502 - 514.

[18] Z. Zhang, G.H. Paulino, Wave propagation and dynamic analysis of smoothly graded heterogeneous continua using graded finite elements. International Journal of Solids and Structures 44 (2007) 3601 - 3626.

[19] M.W. Schraad, F.H. Harlow, A stochastic constitutive model for disordered cellular materials: Finite-strain uni-axial compression. International Journal of Solids and Structures 43 (2006) 3542 - 3568.

[20] ABAQUS User Manual v6.7., 2007 Dassault Systémes.

[21] S. Kiernan, L. Cui, M.D. Gilchrist, A numerical investigation of the dynamic behaviour of functionally graded Foams. IUTAM Symposium on Multi-Functional Material Structures & Systems, Dattaguru (Ed.) Springer pp 15 - 24 (2010).

[22] H.L. Schreyer, Q.H. Zuo, A.K. Maji, Anisotropic plasticity model for foams and honeycombs. Journal of Mechanical Engineering 120 (1994) 13 - 31.

[23] IS. EN 1384: 1996 Specification for helmets for equestrian activities. Dublin, National Standards Authority of Ireland; 1996.

[24] IS. EN 14572:2005: High performance helmets for equestrian activities. Dublin, National Standards Authority of Ireland; 2005.

[25] M.A. Forero Rueda, L. Cui, M.D. Gilchrist, Optimisation of energy absorbing liner for equestrian helmets. Part I: Layered foam liner. Journal of Material and Design 30 3405-3413 (2009).

[26] L. Cui, M.A. Forero Rueda, M.D. Gilchrist, Optimisation of energy absorbing liner for equestrian helmets. Part II: Functionally graded foam liner. Journal of Material and Design 30 3414-3419 (2009).

[27] W.Y. Jung, A.M. Kraynik, S, Kyriakides, On the microstructure of open-cell foams and its effect on elastic properties, International Journal of Solids and Structures 45 (2008) 1845 - 1875.

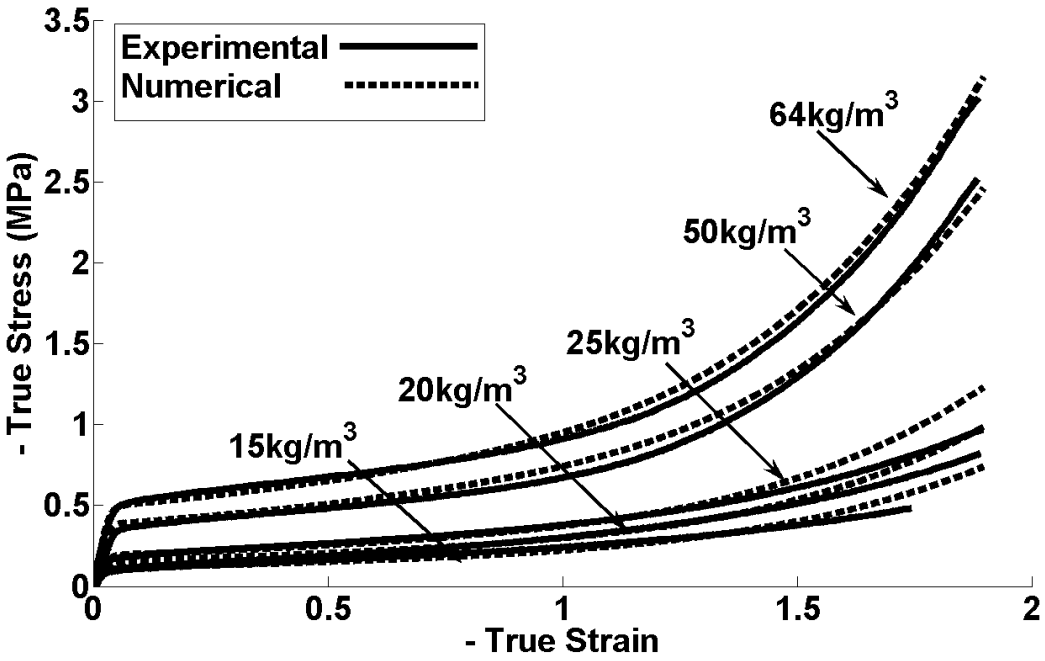

Figure 1: Stress strain response of EPS foams across a range of densities at a strain rate of 0.001/s.

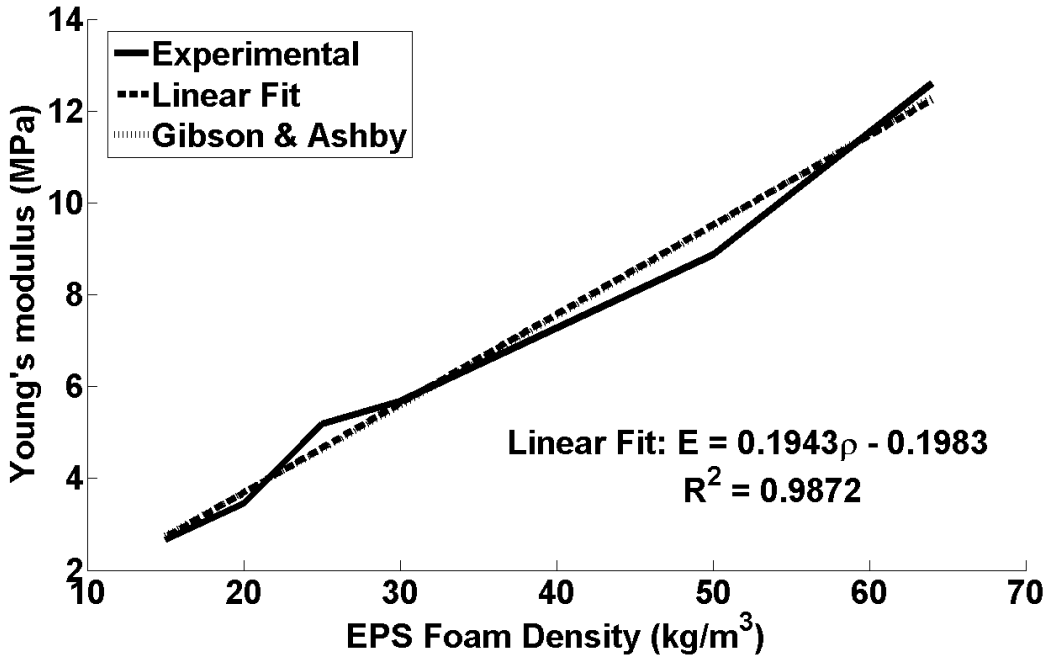

Figure 2: Fitting of Young's modulus as a function of EPS foam density (linear and by Gibson & Ashby)

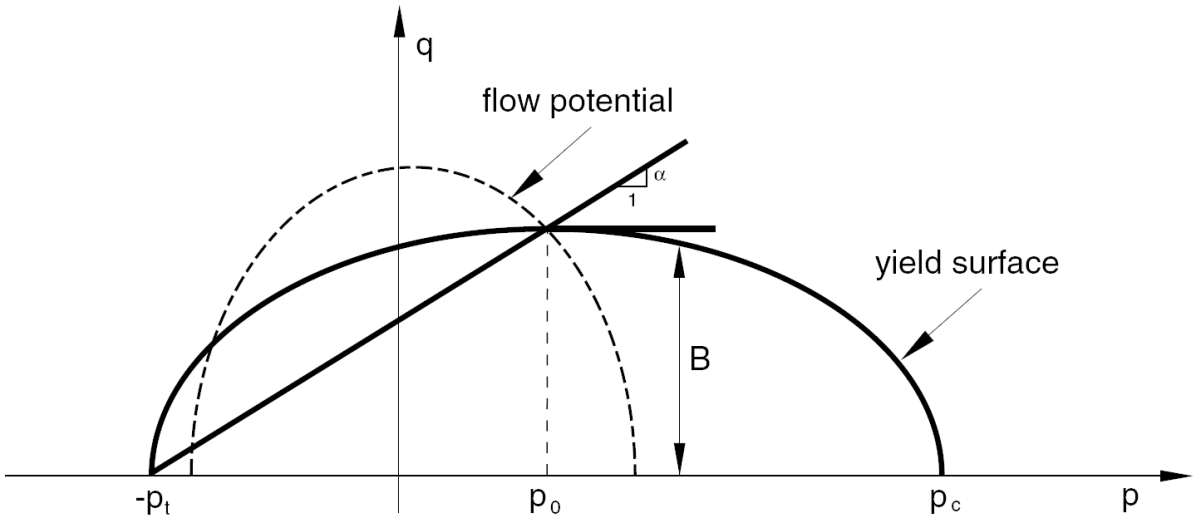

Figure 3: The initial yield surface and flow potential of the ABAQUS crushable foam model. ABAQUS [20]

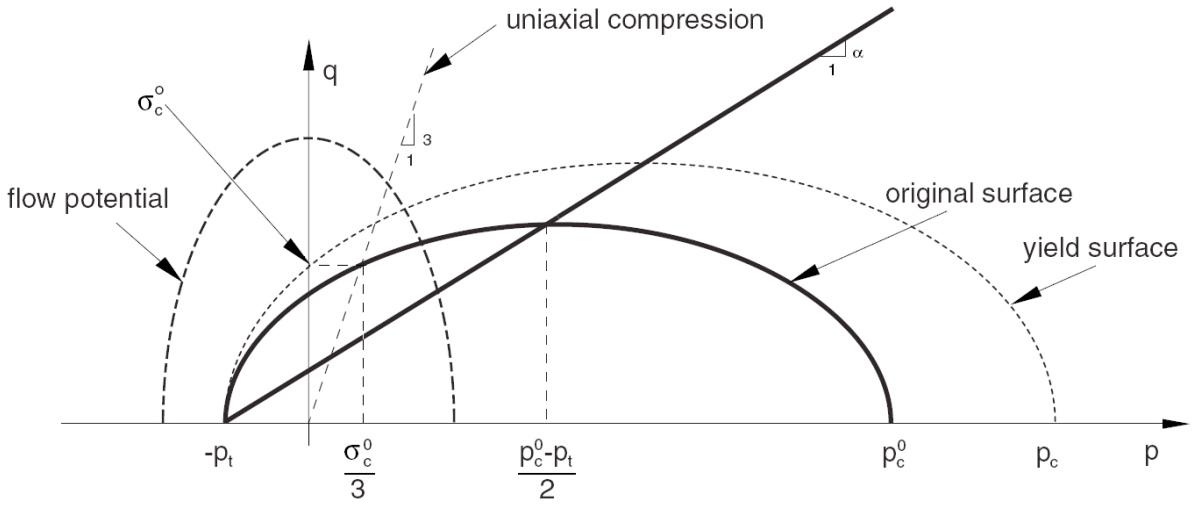

Figure 4: As plastic strain increases p_c increases in size while p_t remains constant, leading to a volumetric expansion of $\partial \mathbb{E}_\sigma$ with plastic strain. ABAQUS [20]

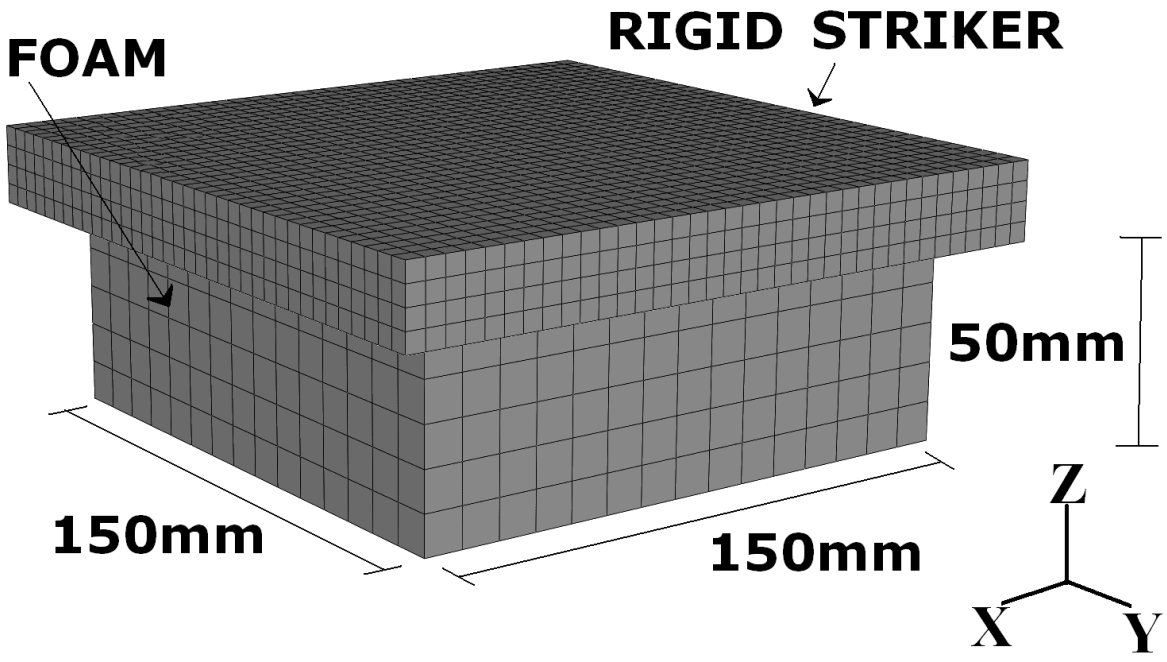

Figure 5: The model assembly used to simulate the dynamic response of a virtual EPS specimen.

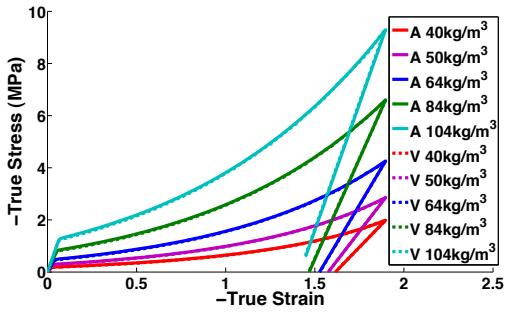

(a) $\sigma - \varepsilon$

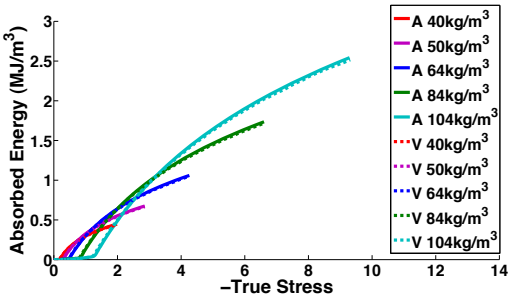

(b) $\psi - \sigma$

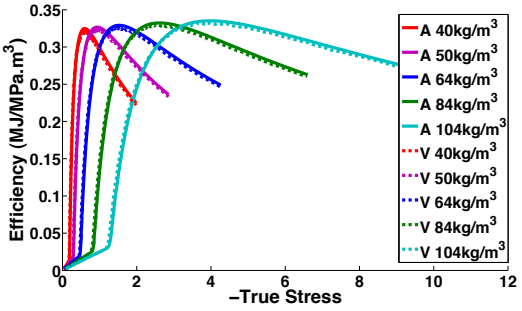

(c) $\varphi - \sigma$

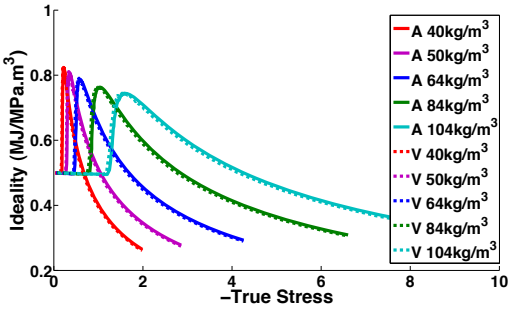

(d) $\iota - \sigma$

Figure 6: Stress - Strain ($\sigma - \varepsilon$), Energy - Stress ($\psi - \sigma$), Efficiency - Stress ($\varphi - \sigma$) and Ideality - Stress ($\iota - \sigma$) static compressive reponse between the `HEX` and `VUMAT` for 40kg/m^3 - 104kg/m^3 foam with a Poisson's ratio of 0.0.

A_0	A_1	A_2	σ_{ε_y}	σ_{ε_D}	ε_y	ε_D
1.3	0.021	0.1	0.015	0.155	0.03	0.89

Table 1: Calibrating parameters for Schraad & Harlow model (64kg/m^3).

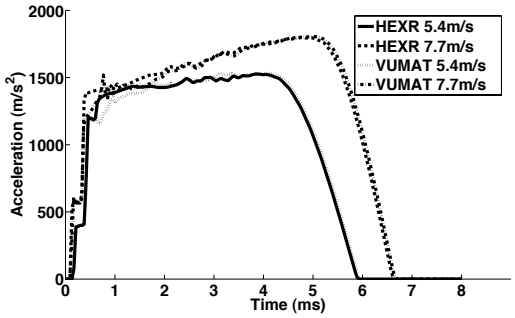

(a) ρ^f = 40kg/m^3

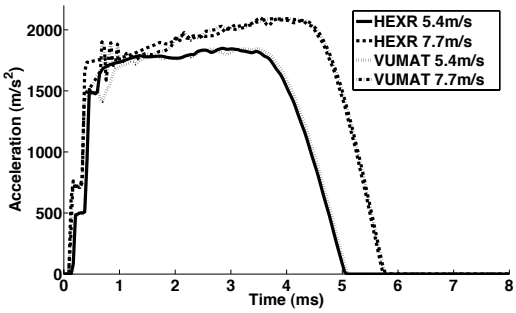

(b) ρ^f = 50kg/m^3

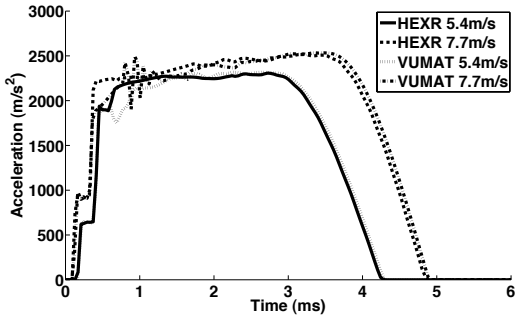

(c) ρ^f = 64kg/m^3

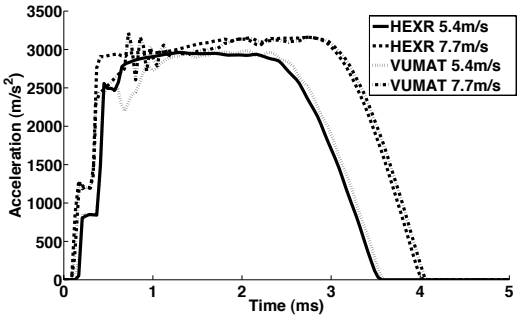

(d) ρ^f = 84kg/m^3

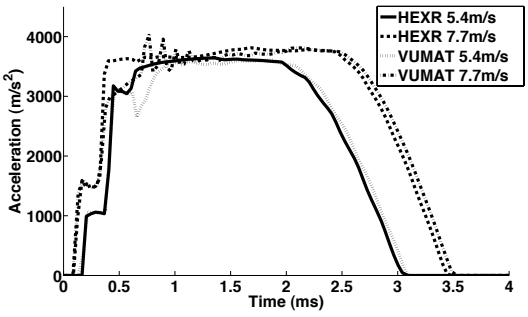

(e) ρ^f = 104kg/m^3

Figure 7: Comparison of acceleration time traces between `HEX` and `VUMAT` for various density foams with a Poisson's ratio of 0.0.

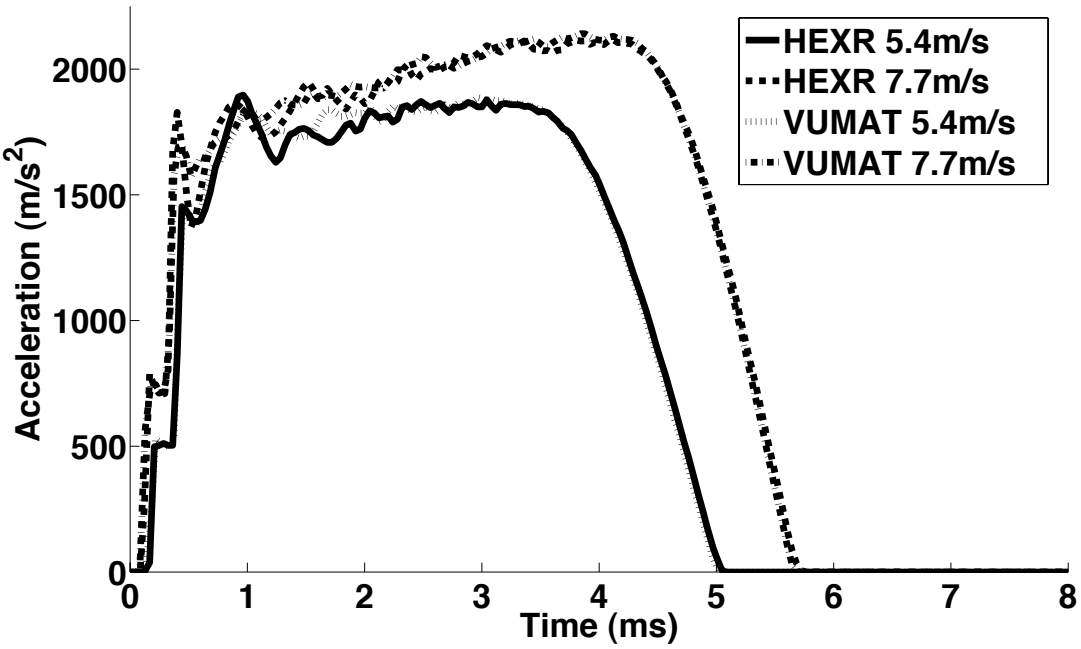

Figure 8: Comparison of acceleration time traces between `HAX` and `VUMAT`for 50kg/m^3 foam with a Poisson's ratio of 0.2.

Foam density (kg/m^3):			40	50	64	84	104
HEX	5.4m/s	$Time_{CPU}$	00:00:07	00:00:07	00:00:07	00:00:06	00:00:06
		Inc_{Stable} (x10^{-5})	1.32	1.31	1.29	1.27	1.26
		$Inc_{No.}$	927	831	746	678	664
	7.7m/s	$Time_{CPU}$	00:00:09	00:00:09	00:00:07	00:00:08	00:00:08
		Inc_{Stable} (x10^{-5})	1.31	1.32	1.31	1.29	1.27
		$Inc_{No.}$	1172	1054	885	796	752
VUMAT	5.4m/s	$Time_{CPU}$	00:40:29	00:33:47	00:30:16	00:27:25	00:28:41
		Inc_{Stable} (x10^{-5})	1.25	1.24	1.22	1.21	1.20
		$Inc_{No.}$	1064	958	873	795	808
	7.7m/s	$Time_{CPU}$	00:52:57	00:41:03	00:34:50	00:30:30	00:27:50
		Inc_{Stable} (x10^{-5})	1.23	1.24	1.23	1.20	1.20
		$Inc_{No.}$	1406	1115	934	851	783

Table 2: CPU Times, Stable time increments and number of increments for 40, 50, 64, 84 and 104kg/m^3 `HEX` & `VUMAT` acceleration management simulations.

	HEX	VUMAT
Input Parameters	ρ^{f} E^{f} υ^{el} $\sigma_{\mathrm{True}} - \varepsilon^{\mathrm{pl}}_{\mathrm{True}}$ curve p_t p_c	ρ^{f}

Table 3: Required input parameters for the HEX and proposed VUMAT (υ^{el} in the VUMAT is assumed to be 0.0, but can be changed internally).